NASA TECHNICAL MEMORANDUM

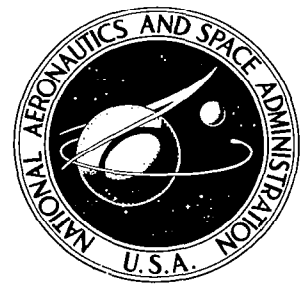

NASA TM X-2371

HEAT-TRANSFER EXPERIMENTS ON A 34-AMPERE-HOUR NICKEL-CADMIUM CELL

by Curt H. Liebert

Lewis Research Center
Cleveland, Ohio 44135

NATIONAL AERONAUTICS AND SPACE ADMINISTRATION • WASHINGTON, D. C. • SEPTEMBER 1971

1. Report No.	2. Government Accession No.	3. Recipient's Catalog No.
NASA TM X-2371		

4. Title and Subtitle	5. Report Date
HEAT-TRANSFER EXPERIMENTS ON A 34-AMPERE-HOUR NICKEL-CADMIUM CELL	September 1971
	6. Performing Organization Code

7. Author(s)	8. Performing Organization Report No.
Curt H. Liebert	E-6391
	10. Work Unit No.
	120-34

9. Performing Organization Name and Address	11. Contract or Grant No.
Lewis Research Center National Aeronautics and Space Administration Cleveland, Ohio 44135	
	13. Type of Report and Period Covered
12. Sponsoring Agency Name and Address	Technical Memorandum
National Aeronautics and Space Administration Washington, D. C. 20546	14. Sponsoring Agency Code

15. Supplementary Notes

16. Abstract

Local transient temperature distributions throughout the plate pack of operating nickel-cadmium cells and accompanying jar temperatures are reported herein for a 34-ampere-hour cell. The cell was charged at 7 amperes and was discharged into the exhaustion region at constant currents ranging from 16 to 68 amperes. Temperature distributions were recorded for a variety of heat-transfer conditions which could be encountered in practical battery applications. At given times, average theoretical temperatures calculated by use of transient lumped heat-transfer models predicted local experimental temperatures within ±4 percent. This suggests that simple lumped theory can be applied with confidence to the thermal design of nickel-cadmium batteries.

17. Key Words (Suggested by Author(s))	18. Distribution Statement
Nickel-cadmium batteries Heat transfer	Unclassified - unlimited

19. Security Classif. (of this report)	20. Security Classif. (of this page)	21. No. of Pages	22. Price*
Unclassified	Unclassified	21	$3.00

* For sale by the National Technical Information Service, Springfield, Virginia 22151

HEAT-TRANSFER EXPERIMENTS ON A 34-AMPERE-HOUR NICKEL-CADMIUM CELL

by Curt H. Liebert

Lewis Research Center

SUMMARY

To date, no experiments have been performed that evaluate the local transient temperature distributions throughout the plate pack of operating nickel-cadmium cells. Such temperature distributions and accompanying jar temperatures are reported herein for a 34-ampere-hour cell. The cell was charged at 7 amperes and was discharged into the exhaustion region at constant currents ranging from 16 to 68 amperes. Temperature distributions were recorded for a variety of heat-transfer conditions that could be encountered in practical battery applications.

At given times, average theoretical temperatures calculated by use of transient lumped heat-transfer models predicted local experimental temperatures within ±4 percent. This suggests that simple lumped theory can be applied with confidence to the thermal design of nickel-cadmium batteries.

INTRODUCTION

Heat-transfer models that can be applied to the thermal design of flight batteries are useful to battery design engineers. The space program has contributed much to the methods of the thermal design of nickel-cadmium cells and batteries operating at relatively low charge and discharge currents and at relatively short discharge times (ref. 1). Publications dealing with the more severe heat-transfer problems associated with discharging these cells over long periods at high currents and at correspondingly higher rates of internal heat generation are not available. This report contributes data and theory to this area.

The theoretical and experimental rates and mechanisms of internal heat generation associated with the electrochemical reactions within many types of cells during charge and discharge have been extensively investigated (refs. 2 to 9). With the rate of internal

heat generation known, the temperature of the cell can be predicted using theoretical heat-transfer models presented in the literature. Some of these models assume that the temperature varies with time but is not space dependent. Such lumped models are presented in references 4 and 6. They predict an average temperature at a prescribed time. Other models, composed of partial differential equations, assume that the temperature is both space and time dependent and are therefore based on more complex formulations (refs. 8 and 9). References 4, 6, and 9 also apply Newton's law of cooling for predicting the amount of heat that can be transferred from the outer wall of the cell jar to the surroundings.

Reported herein are the transient temperature, voltage, and current data for an operating 34-ampere-hour, nickel-cadmium cell, which was alternately charged at 7 amperes, the highest charge rate suggested by the manufacturer, and discharged at constant currents of 16, 30, 50, and 68 amperes.

The cell was operated using both passive and active cooling techniques. In the passive cooling technique, data were taken when the cell was insulated with glass wool and when the bare cell was operated in still air. This condition approximates heat transfer from cells placed in a container to form a battery. The active cooling experiments were done by operating the cell with air blowing (forced convection) over the two broad sides, over the two narrow sides, or over one broad side while the other surfaces were insulated.

Temperatures of batteries used in space vehicles are usually controlled by attaching them to an actively cooled plate (or fins) with heat transferred from the cell to the plate by conduction. Although this method for transferring heat differs from the forced-convection tests described herein, the physics of internal heat transfer within the cell are identical. Also, Newton's law for external cooling is valid for both methods. This law states that the heat transferred is proportional to the temperature gradient normal to the direction of heat flow. For convection, the proportionality coefficient is defined as the heat-transfer coefficient. The proportionality coefficient may be approximated by the ratio of the medium thermal conductivity to the thickness when cooling is by conduction. Thus, the results of the forced-convection experiments can be applied to the cooling of flight batteries.

Local transient temperatures of the outer jar wall and throughout the plate pack were measured as the cell was being charged and as the cell was almost totally discharged into the exhaustion region. These measurements are unique because, to date, no data can be found in the literature of measurements of the actual local temperature distributions within the plate pack of operating nickel-cadmium cells. The data were averaged and compared with calculated values of cell temperatures based on simple, lumped, heat-transfer models.

EXPERIMENT

Cell Construction and Operation

A General Electric vented plastic jar, 34-ampere-hour cell (catalog number 43B034AC01) was used in these tests. The general construction of the cell is given in "Operating and Service Manual for General Electric Nickel-Cadmium Vented Cell Batteries" published by the General Electric Company.

The cell was charged at a constant current of 7 amperes to 140 percent of the previous ampere-hour discharge. Then the cell was discharged through a constant current load at 16, 30, 50, and 68 amperes. Charge and discharge time, current, and closed-circuit voltage were monitored. Voltage and current measurement error was less than 1 percent.

The charge and discharge cycling were not continuous. The cell remained on open circuit (shutdown) between cycles. When the cell was on open circuit, it spontaneously discharged with a resulting decrease in voltage (self-discharge). If the charging process was interrupted and the cell placed on open circuit for any extended period, the voltage was noted at the beginning of the open-circuit period. Then, following the nonoperating period, the cell was charged at 7 amperes to the voltage recorded at the beginning of the previous shutdown time before continuing the charge to 140 percent of the previous ampere-hour discharge. In this way, the ampere-hours lost by the cell during self-discharge were approximately replaced.

Thermocouples

Nine Chromel and Constantan thermocouples were placed in the plate pack of 31 electrodes (fig. 1). This type of thermocouple was used because it is compatible with the electrolyte used in these tests (KOH and distilled water) and because the variation of electromotive force output with temperature is the largest of all commonly used thermocouples. The Chromel and Constantan wires were covered with Teflon. The outside diameter of each wire was 0.025 centimeter (0.10 in.) The placement was such that the temperature differences along the length and width of the pack could be recorded. Three thermocouples each were placed between the first and second, 15th and 16th, and 30th and 31st electrodes. Six Chromel and Constantan thermocouples (0.01-cm-diam wire) were also attached to the outside of the jar wall at the positions shown in figure 1. Bulk cooling air temperatures were also measured. An ice bath was used as the reference junction for the thermocouple system and millivolt readings were obtained with a 24-channel multipoint recorder.

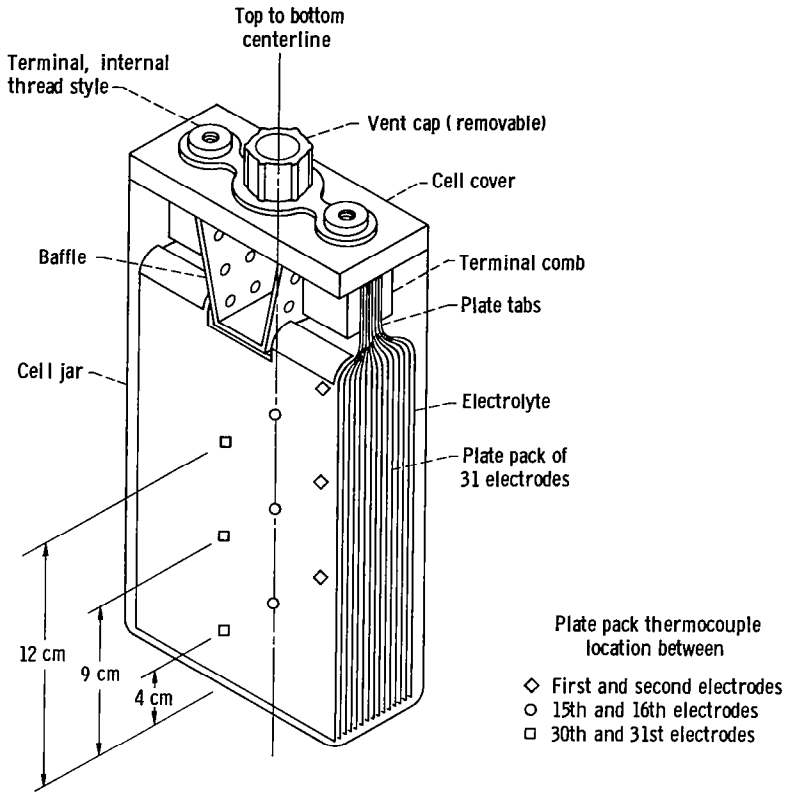

Figure 1. - Construction of nickel-cadmium vented-cells and location of thermocouples in plate pack. Note: there are three jar thermocouples on each side adjacent to the pack thermocouple location.

The thermocouples used to measure bulk cooling air temperature were calibrated in heated water at temperatures varying from 298 to 400 K and then positioned on the apparatus.

Conversely, the cell thermocouples were calibrated after they were attached to the cell. These calibrations spanned a temperature range of 298 to 315 K. This was accomplished by placing the cell in a constant temperature oven. After the cell reached equilibrium, mercury thermometer temperature readings accurate to ±0.5 K were recorded outside the cell and were compared with the thermocouple readings of the cell.

Thermocouple calibrations were done before and after the electrolyte was added to the cell, but before the initial charging which produced an electrical field within the cell. Also, calibrations were taken during the charging mode but before times corresponding to oxygen recombination. (As will be discussed later, the cell temperature rises slightly during oxygen recombination.) Thermometer and thermocouple readings always agreed with 0.5 K, indicating that the electrical field was not adversely affecting the thermocouple readings.

Cell thermocouple junctions were in direct contact with the electrolyte for a period of about 6 months. During this time thermometer and thermocouple calibrations always

agreed within 0.5 K. This good agreement indicated that the caustic electrolyte was not adversely affecting thermocouple performance.

According to the manufacturer, a voltage below 1.5 volts or above 1.65 volts during constant current overcharge indicates that the cell is not performing properly. During overcharge the voltage of the cell investigated herein varied from 1.59 to 1.62 volts. Thus the installation of the thermocouples had no apparent effect on cell performance.

Heat-Transfer Conditions and Analysis

Five heat-transfer conditions were examined.

Case I (passive cooling) includes results for (a) the cell wrapped in glass wool to a thickness of about 91 centimeters (3 ft), (b) the cell surrounded by a 7.62-centimeter (3-in.) layer of air with this system then insulated with about 91 centimeters (3 ft) of glass wool.

Case II (active cooling) presents results for the cell cooled by forced-air convection on the exterior of (a) two broad jar sides, (b) two narrow sides, and (c) one broad side.

The forced-convection cooling was accomplished with the tunnel apparatus shown in figure 2. The cell and tunnel walls formed rectangular ducts through which turbulent air

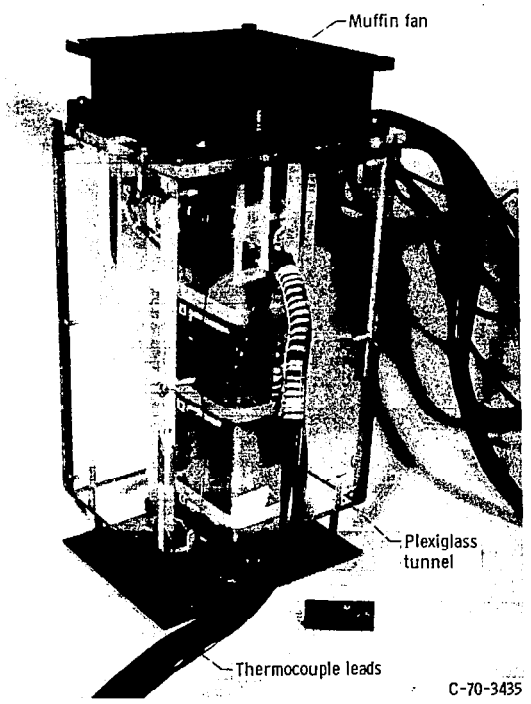

Figure 2. - Heat-transfer apparatus.

was forced by a muffin fan. According to the manufacturer, this fan has a flow rate of 47 195 cubic centimeters per second (100 ft^3/min). The fan could not be conveniently calibrated, but other calibrations with similar fans indicated that this rate is accurate to ±2 percent. The outside of the Pyrex tunnel wall was insulated with glass wool (not shown) at a thickness of 91 centimeters (3 ft). The bulk cooling air temperature T_∞ was measured with Chromel and Constantan thermocouples (0.01-cm-diam wire) placed about 0.2 centimeter from the inside tunnel wall.

Lumped heat-transfer models were formulated for predicting the transient temperatures measured for the conditions and were compared with experiment. The analysis is presented in appendix A.

RESULTS AND DISCUSSION

The data presented in figure 3 illustrate the trends in the transient variations of voltage and temperature observed for the heat-transfer cases. The voltage trends are in accord with those presented in the literature and indicate that the cell is performing as expected.

As the cell was operated, cell voltages always decreased during discharge and increased to about 1.62 volts during charge (fig. 3). The relatively more rapid voltage rise, which occurred some time after the start of charge (210 min) is well known in nickel-cadmium cells and is associated with the oxygen evolution recombination cycle. Bubbles were noted in the liquid electrolyte during this period.

Plate pack and jar temperatures increased during discharge and decreased during charge until significant oxygen recombination was encountered, after which time the temperatures rose about 1 K and then remained essentially constant (fig. 3). The small temperature rise is the result of heat generation within the cell which is produced by oxygen recombination. Because this temperature increase is small, the theoretical analysis presented herein assumes that the heat of recombination is negligible.

During operation, temperature variations were noted throughout the volume of the cell; thus, models based on partial differential equations could be used to predict each local temperature as a function of time and space. However, the thermal conductivity must be known when evaluating the temperature given in the equations derived from such distributed parameter models. According to reference 10, this property is not well known. Also, an evaluation of internal cell dimensions is difficult. Thus, large calculation inaccuracies are possible. Therefore, for engineering purposes, use of models based on partial differential equations is not required if simple, lumped models can be applied that predict a temperature at a specified time which is in reasonable agreement with the actual spatial temperatures.

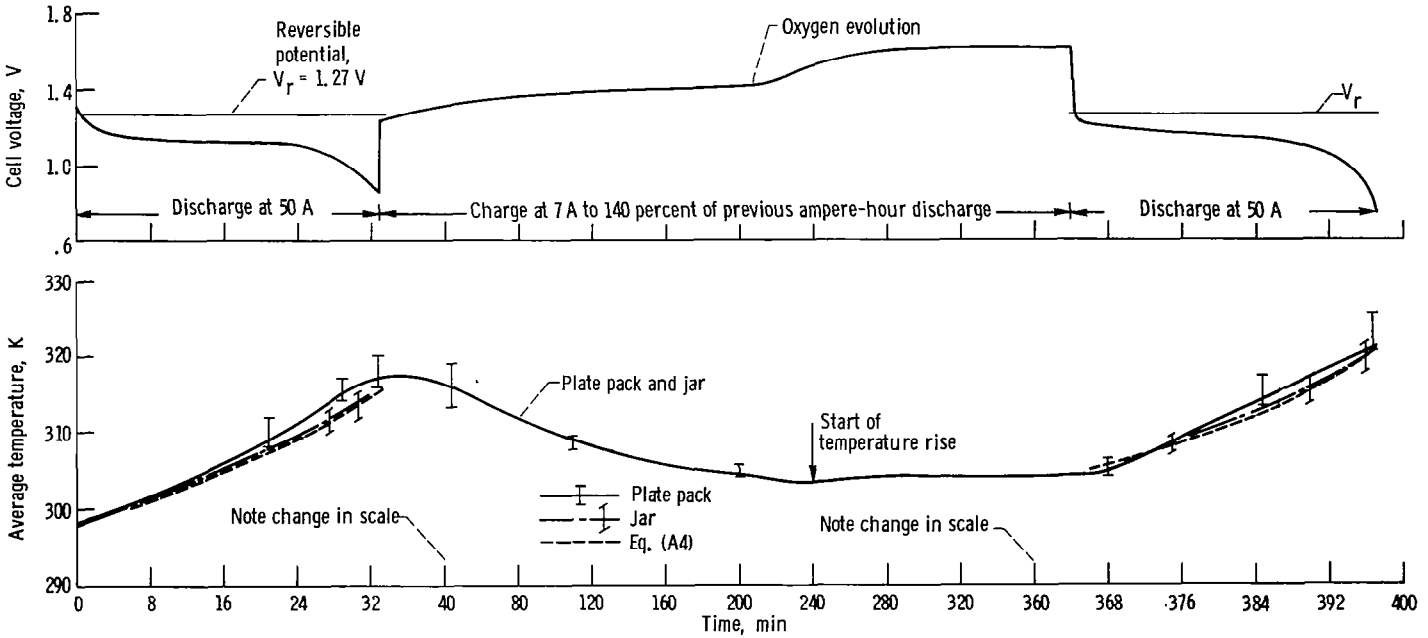

Figure 3. - Case I(a). Voltage and average temperature against time for insulated cell. Discharge current, 50 amperes.

Lumped heat-transfer models, presented in appendix A, are based on the specific heat of the cell. For nickel-cadmium cells, the reported specific heats of 19 cells vary between about 0.8380 to 1.592 joules per gram per K (0.20 to 0.38 cal/(g)(K)), with a calculated average of about 1.131 joules per gram per K (0.27 cal/(g)(K)) (ref. 10). This leads to an uncertainty of the calculated temperature of about ±5 percent.

Case I(a)

The curves in figures 3 and 4 present the voltage, the average temperature data for the plate pack, and the average temperature of the insulated jar at discharge currents of 16, 30, 50, and 68 amperes. The voltage and current were not recorded continuously. But 10 to 15 data points were taken during the discharge period, and an equal number of points were taken during charge. The data at a given time were averaged and a smooth line was drawn through the variation of voltage and temperature with time.

The bars shown at selected measurement times (figs. 3 and 4) represent the range of temperatures. The upper and lower portion of the bar coincides with the highest and lowest temperature. The highest temperatures occurred along the top to bottom centerline of the plate pack. Side electrode (bottom portion of the bar) and jar wall temperatures were about 2 and 3 percent lower, respectively, than the hot-spot temperatures.

Comparison of experimental plate-pack temperatures and jar temperatures with electrochemical discharge theory (ref. 3) using equation (A4) are also presented in figures 3 and 4. In figure 3 this comparison is made for two discharge regimes. Experiment agrees with theory to within ±3 percent over a broad range of discharge current, voltage, and temperature.

Case I(b)

The cell was also tested in still air. The temperature trends were identical to those found in case I(a). The theory for case I(a) was also applied at discharge to this case. The experiment agreed with the theory within ±4 percent. The experimental agreement with a theory based on insulated conditions was expected as it is known that air is a good insulator.

Case II(a) (Discharge)

Figure 5 presents the average plate pack and average jar wall temperatures of the

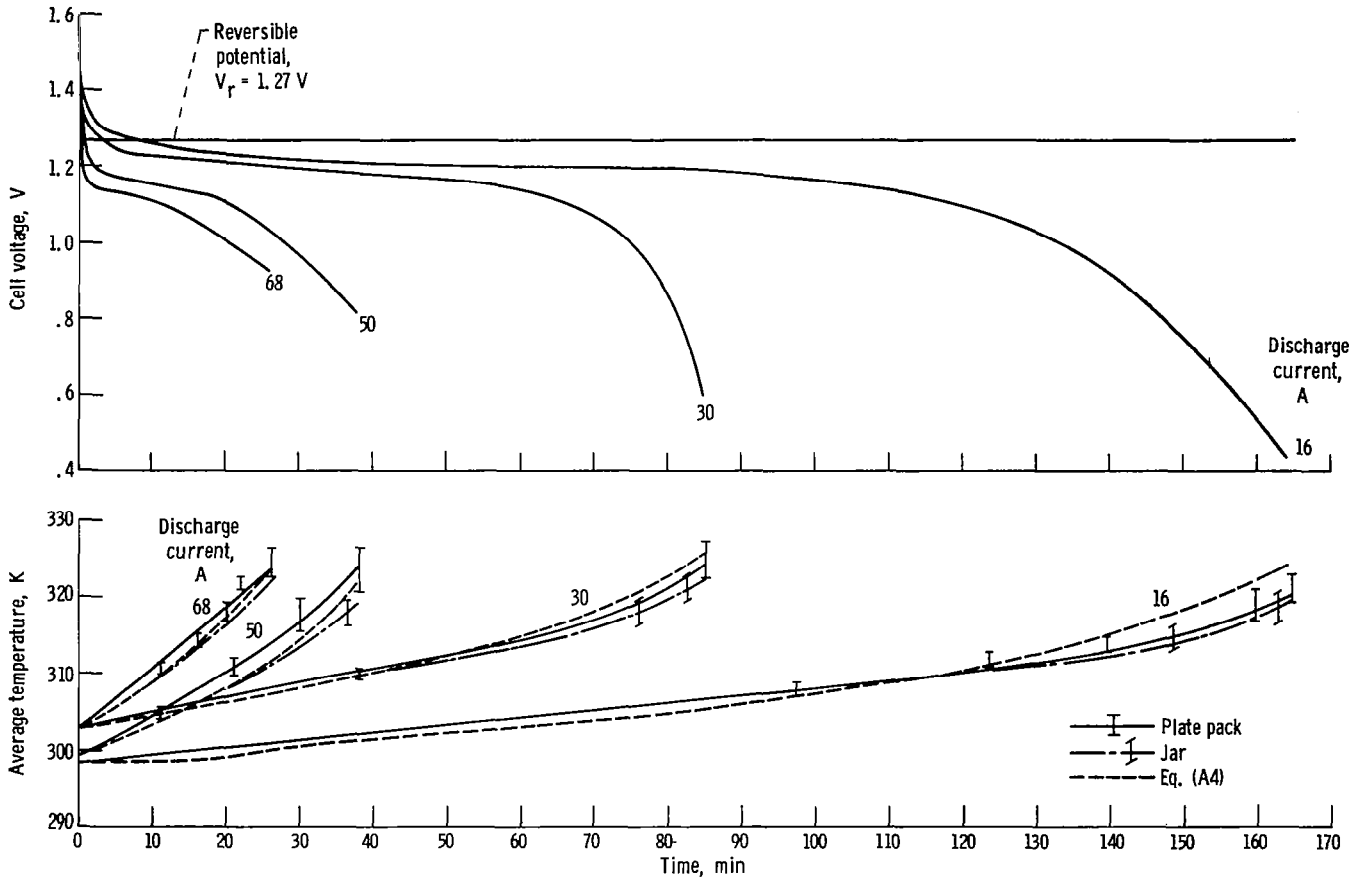

Figure 4. - Case I(a). Voltage and average temperature against time for insulated cell.

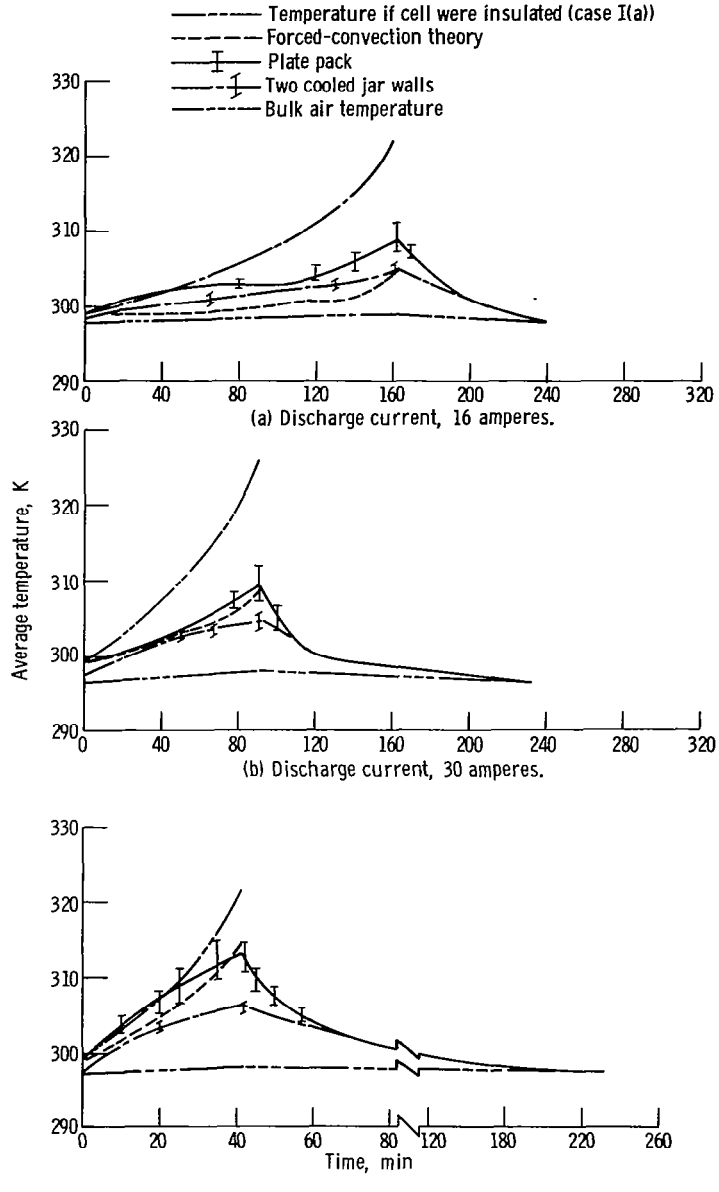

Figure 5. - Case II(a). Cooling to both large sides of cell.

cell cooled on both broad sides by forced convection. The bulk cooling air temperature is also given. The narrow side, top, and bottom of the cell were insulated. The cell was discharged at 16, 30, and 50 amperes. Also shown is the calculated temperature of the cell if it were insulated with glass wool (eq. (A4)). As expected, the cell temperature has been substantially lowered by forced-convection cooling. The highest temperatures randomly occurred along the top to bottom centerline of the plate pack. Side electrode and wall temperatures were 2 and 4 percent lower, respectively, than hot-spot temperatures. The bulk cooling air temperature and ambient temperature were always identical at the start of discharge. The bulk cooling air temperature rose about 2 K above ambient temperature at the end of discharge and decreased to ambient as the cell was charged.

The model derived for this heat-transfer condition, unlike that used to predict the cell temperature of case I, includes Newton's law of cooling (eq. (A6)). This law defines the heat transfer by convection as proportional to the difference between the jar wall temperature and bulk air temperature. The porportionality coefficient is the heat-transfer coefficient. The theoretical curves presented in figure 5 predict plate pack and jar temperatures within ±3 percent.

Case II(a) (Charge)

In practice, it may be useful to calculate the length of time needed to reduce the battery temperature at the end of discharge to ambient. This time will be defined herein as cooling time. The cooling time in figure 5(a), for instance, is given as that time between 162 and 240 minutes or 1.3 hours.

Table I presents a comparison of experimental and theoretical cooling time to am-

TABLE I. - CELL COOLING TIME TO AMBIENT TEMPERATURE DURING CHARGE AT 7 AMPERES

Case	Figure	Experimental cooling time, hr	Theoretical cooling time, hr
II(a)	5(a)	1.3	1.3
	5(b)	2.4	2.1
	5(c)	3.2	3.3
II(c)	6(a)	3.3	2.9
	6(b)	3.1	3.1
	6(c)	3.2	3.1

bient. The theoretical cooling time was calculated using equation (A8) and was derived assuming, again, a lumped model and no heat of oxygen recombination. Experiment compares with theory within ±14 percent.

Case II(b)

The cell was also cooled on both narrow sides by forced convection with the broad faces insulated. The cell was charged at 7 amperes and discharged at 16 and 30 amperes. Cell pack and wall temperatures and bulk-air temperatures were recorded. The theory of case II(a) (charge and discharge) was applied. As was observed for case II(a), the experimental temperatures agreed with theoretical temperatures within ±3 percent during discharge, and experimental cooling times were within ±15 percent of theoretical during charge.

Reference 10 indicates that the plate-pack thermal conductivity of nickel-cadmium cells is anisotropic. A review of general cell construction shows that the heat-transfer path along the metal electrode to narrow faces should offer far less resistance than that normal to the electrode faces. The theory presented in cases II(a) and (b) is derived from the same model and does not take anisotropy into account. The experimental results are in reasonable agreement with theory for both cases. If anisotropy were a large effect, it is not likely that theory and experiment would agree so well for heat transfer from both the broad and narrow sides.

The effect of anisotropy may be negated by interior cell construction. The outermost electrodes are in contact with a layer of separator material, which is in direct contact with the broad jar walls. However, the plate pack is separated from the narrow walls by several layers of folded separator material and electrolyte over a distance of about 0.25 centimeter (0.1 in.). Thus, heat transfer from pack to narrow walls will be poor compared with heat transfer from pack to broad walls because distances from pack to narrow walls are much greater.

Case II(c) (One Large Heat-Transfer Area)

Figure 6 presents the average temperature of the plate pack and the insulated broad face for the cell as it was cooled on one broad side and insulated on the other five sides. Also shown is the average temperature of the cooled wall and the bulk-air temperature. Contrary to case II(a), the highest temperatures measured occurred randomly in the volume located between the top to bottom plate pack centerline and the insulated walls. Other cell temperatures were within 4 percent of the hot-spot temperature. The lumped

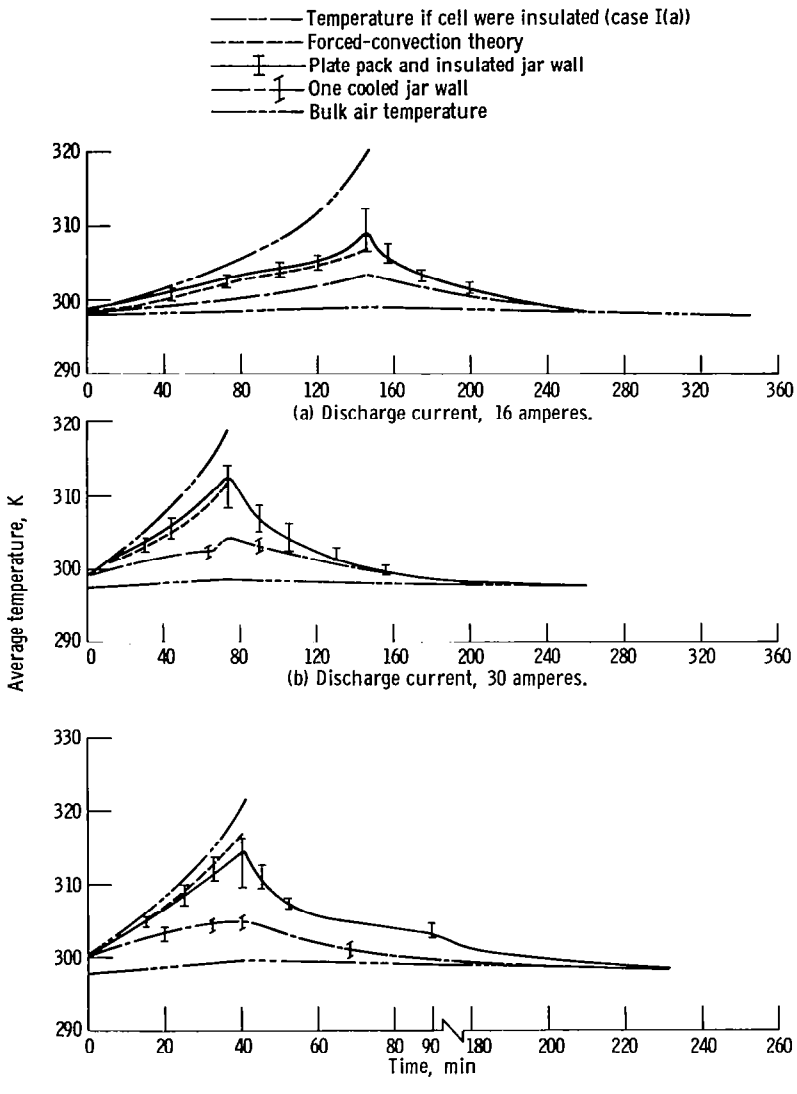

Figure 6. - Case II(c). Cooling to one large side of cell.

theory derived for case II(a) was also applied to this case and experimental cell temperatures were within ±4 percent of theoretical values. Comparison of experimental and theoretical cooling times is given in table I. Experiment compares with theory within 14 percent.

CONCLUDING REMARKS

To date, no experiments are known that evaluate the local temperature distributions throughout the plate pack of operating nickel-cadmium cells. While models based on partial differential equations could be applied to predict the local cell temperatures, use of such models may not be warranted if more simple and less rigorous lumped models can be applied that predict temperature-time relations in reasonable agreement with the actual cell temperatures.

Temperature distributions along the length and width of the pack and also along the length of the jar wall of a 34-ampere-hour cell are reported herein. Temperatures were recorded when the cell was subjected to various simulated heat-transfer conditions similar to ones that could be encountered in practical design problems.

The highest temperatures were found in the plate pack and varied in location with heat-transfer conditions. Other temperatures measured on the jar walls and throughout the pack were within 4 percent of the highest temperatures.

Theoretical temperatures calculated herein by use of lumped models predicted experimental temperatures within ±4 percent. The good agreement of theory and experiment over broad ranges of discharge current and voltage and heat-transfer conditions suggests that the theory can be applied with confidence to the thermal design of nickel-cadmium batteries when the heat of oxygen recombination is negligible.

Lewis Research Center,
National Aeronautics and Space Administration,
Cleveland, Ohio, July 6, 1971,
120-34.

APPENDIX - HEAT BALANCE EQUATIONS AND CALCULATION PROCEDURE

Case I(a) (insulated cell). - The heat generated irreversibly at constant temperature and pressure within a cell on discharge is given by reference 3 as

$$q_t = \int I(V_r - V)dt + T\Delta S \tag{A1}$$

where

q_t heat internally generated, J

I current, A

V_r reversible potential, V

V working cell terminal potential, V

t time, sec

T temperature, K

ΔS entropy, J/(g)(equiv K)

This may be written for the discharging nickel-cadmium system as

$$q_t = 60 \int_0^{\theta} I(1.27 - V)d\theta' + 383.4(AH)_{\theta} \tag{A2}$$

where

(1.27 - V) reversible cell potential (ref. 2) minus working cell terminal potential, V

θ discharge time, min

383.4 enthalpy change minus molar Gibbs free-energy change (ref. 3), J/A-hr

$(AH)_{\theta}$ ampere-hour discharge from time zero to time t

The heat stored, $mc(T_{\theta} - T_0)$, equals the heat internally generated. Thus, for constant current,

$$mc(T_{\theta} - T_0) = 60I \int_0^{\theta} (1.27 - V)d\theta' + 383.4(AH)_{\theta} \tag{A3}$$

where

m	mass of cell, g
c	specific heat of cell, J/(g)(K)
$(T_\theta - T_0)$	temperature at a given discharge time minus temperature at zero discharge time, K

The mass for the cell investigated herein is 1420 grams. Reference 10 reports that the average specific heat of nickel-cadmium cells is about 1.131 joules per gram per K (0.27 cal/(g)(K)) and does not vary significantly with cell size, weight, ampere-hour capacity, and direction of measurement. This value of specific heat was averaged from data given for 19 cells with capacities of 5 through 75 ampere-hours.

Substituting these values of m and average c into equation (A3) yields

$$T_\theta - T_0 = 0.0374I \int_0^\theta (1.27 - V)d\theta' + 0.239(AH)_\theta \tag{A4}$$

This equation was used to calculate T_θ at five values of time for the various correlated test conditions (figs. 3 and 4). A smooth line was drawn through the five calculated points.

Case II(a), (b), and (c) (discharge). - On discharge, the net heat in the cell q_{net} equals the heat internally generated minus the heat transferred to the surroundings:

$$q_{net} = mc(T_\theta - T_0) = \left[60I \int_0^\theta (1.27 - V)d\theta' + 383.4(AH)_\theta\right] - hA \int_0^\theta (T_w - T_\infty)d\theta' \tag{A5}$$

Solving for $T_\theta - T_0$ gives

$$T_\theta - T_0 = \left[0.0374I \int_0^\theta (1.27 - V)d\theta' + 0.239(AH)_\theta\right] - \frac{hA}{1606} \int_0^\theta (T_w - T_\infty)d\theta' \tag{A6}$$

where

h	average heat-transfer coefficient, J/(min)(cm^2)(K)
A	heat-transfer area of plate pack projected normally onto jar wall equal to 210 and 105 cm^2 for cases II(a) and (c), respectively
T_w	wall (jar) temperature, K
T_∞	average bulk cooling air temperature, K

q_{net} net heat remaining in cell at time θ, J

The Reynolds number for these experiments was greater than 10 000, and thus the heat-transfer coefficient may be estimated from the relation (ref. 12)

$$h = 0.023C\frac{k}{D_e}\left(\frac{V'D_e\rho}{\mu}\right)^{0.8}\left(\frac{c_p\mu}{k}\right)^{0.4} \tag{A7}$$

where

C average shortness factor (ref. 12), equal to 1.67 and 1.79 for cases II(a) and (c), respectively

k thermal conductivity of air at T_∞, J/(min)(cm^2)(K)/cm

D_e equivalent diameter $4r_h$, equal to 11.8 and 5.9 cm for cases II(a) and (c), respectively

r_h hydraulic radius, flow cross sectional area/perimeter, cm

ρ density of air at T_∞, g/cm^3

μ viscosity of air, g/(min)(cm)

c_p specific heat at constant pressure of air at T_∞, J/(g)(K)

V' velocity of air, cm/min

The velocity was calculated by dividing the fan flow rate by the flow cross-sectional area. The flow cross-sectional area was 79 and 39 square centimeters for cases II(a) and (c), respectively. For convenience, the apparatus shown in figure 2 was built with a ratio of flow length to effective diameter of about 1 at the inlet to 4 at the outlet on each side. These ratios are much smaller than the ratio of 40 to 60 necessary for fully developed flow, thus the shortness factor C should be included in the Dittus-Boelter equation (eq. (A7)). These factors were computed from equations presented in reference 12 and are closely substantiated by recent data presented in reference 13. Figure 2 shows that the jar walls are not aerodynamically smooth, but it was experimentally determined herein that the protrusions (thermocouples and straps) had no effect on the results. The uncertainty in the values of h calculated herein is believed to be about ±20 percent.

Case II(a), (b), and (c) (charge). - The theoretical cooling times presented in table I were calculated from a heat balance that equates the value of the heat in joules remaining in the cell at the end of discharge (as determined from eq. (A5)) to $60\ hA(T_w - T_\infty)_c t_c$; that is,

$$t_c = \frac{\text{heat remaining at end of discharge}}{60hA(T_w - T_\infty)_c} \tag{A8}$$

where

t_c cooling time during charge needed to reduce plate pack temperature to ambient, hr

$(T_w - T_\infty)_c$ average integrated value over t_c, K

SAMPLE CALCULATION

For case II(a) (cooling to both large sides of cell during charge and discharge), calculate the value of the temperature T_θ at the end of discharge at 50 amperes (fig. 5(c)), and calculate the cooling time t_c, to ambient temperature during charge (table I).

Figure 7 shows the transient variations of voltage for cases II(a) and (c). The area between V_r and V corresponding to 50 amperes shown in figure 7(a) by the cross-

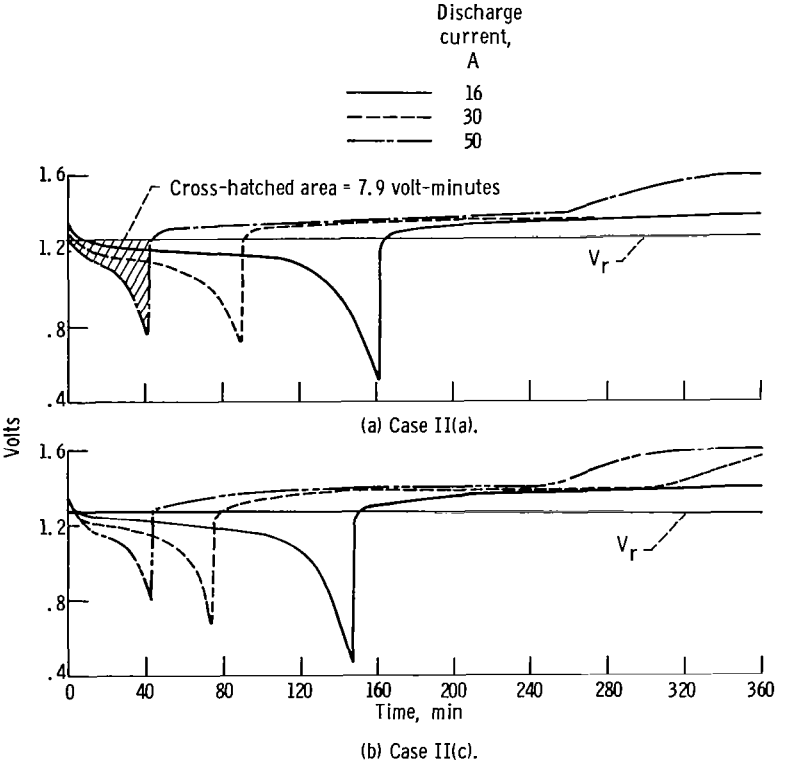

Figure 7. - Variation of voltage with time.

hatched area represents the value of $\int_0^{42} (1.27 - V)d\theta'$ and was determined with a planimeter as 7.9 volt-minutes. Thus, the first term in the brackets of equation (A6) becomes 14.8 K. The second term in the brackets is 8.4 K, and the total of these terms is 23.2 K.

Consider now the second (unbracketed) term in equation (A6). The value of hA was calculated to be (56.77 J/(min)(K)) and hA/1606 is 0.035 1/minute. Values of $T_w - T_\infty$ were calculated from the data of figure 5(c). Plots of $T_w - T_\infty$ against discharge time were drawn and values of $\int_0^{\theta} (T_w - T_\infty)d\theta'$ were determined with a planimeter. For conditions of this example, the value of this integral is 226.8 K-minute and thus the value of the unbracketed term is 7.9 K. Therefore, $T_\theta - T_0 = 15.3$ K. The average experimental temperature of plate pack and wall at the start of discharge T_0 is 299 K and, thus, $T_\theta = 314.3$ K.

Equation (A8) was used to calculate T_c. The heat remaining in the cell at the end of discharge (A5) is $mc(T_\theta - T_0)$, that is, (1606)×(15.3), which equals 24 572 joules. The average value of $(T_w - T_\infty)_c$ found during charge was 2.2 K. This temperature was determined by evaluating the area between the abscissa and a curve representing the values of $T_w - T_\infty$ from 42 to 232 minutes (fig. 5(c)) with a planimeter and then dividing by the experimental cooling time during charge equal to 190 minutes. The value of hA equals 56.77 J/(min)(K), so $t_c = 3.3$ hours.

REFERENCES

1. Thierfelder, H.; and Wylie, T.: Thermal and Mechanical Design of Nickel Cadmium Aerospace Batteries. Space Systems and Thermal Technology for the 70's. Part 1. ASME, 1970.
2. Caulder, Stanley M.: Thermodynamic Properties of the Nickel-Cadmium Alkaline and Lead-Lead Oxide Acid Cells. Ph.D. Thesis, Polytechnic Inst. Brooklyn, 1968.
3. Bauer, Paul: Batteries for Space Power Systems. NASA SP-172, 1968.
4. Gross, Sidney: Heat Generation in Sealed Batteries. Intersociety Energy Conversion Engineering Conference. Vol. 1. IEEE, 1968, pp. 38-46.
5. Gandel, M. G.; and Kinsey, R. H.: Heat Dissipation of Primary and Secondary Batteries. J. Spacecraft Rockets, vol. 2, no. 6, Nov.-Dec. 1965.
6. Schulman, Irwin M.: Secondary Batteries for Energy Storage in Space. Energy Conversion for Space Power. Vol. 3 of Progress in Astronautics and Rocketry. Nathan W. Snyder, ed., Academic Press, 1961, pp. 479-496.
7. Eicke, W. G., Jr.: The "Vicious Cycle" in Secondary Batteries - A Mathematical Approach. J. Electrochem. Soc., vol. 109, no. 5, May 1962, pp. 364-368.
8. Meredith, R. E.; and Uchiyama, A. A.: Theoretical Evaluation of Hot Spot Temperature of Silver-Zinc Batteries. Intersociety Energy Conversion Engineering Conference. Vol. 1. IEEE, 1968, pp. 32-37.
9. Brooman, Eric W.; and McCallum, John: Heat Transfer in Sealed Nickel-Cadmium Spacecraft Cells and Batteries. Battelle Memorial Institute (AFAPL-TR-69-21, AD-851880), Apr. 30, 1969.
10. Brooman, Eric W.: An Annodated Bibliography of the Thermal Properties of Primary and Secondary Cells. Battelle Memorial Institute (AFAPL-TR-70-34, AD-871108), June 1970.
11. Worthing, Archie G.; and Halliday, David: Heat. John Wiley & Sons, Inc., 1948.
12. McAdams, William H.: Heat Transmission. Third ed., McGraw-Hill Book Co., Inc., 1954.
13. Tan, H. M.; and Charters, W. W. S.: Effect of Thermal Entrance Region on Turbulent Forced-Convective Heat Transfer for an Asymmetrically Heated Rectangular Duct with Uniform Heat Flux. Solar Energy, vol. 12, no. 4, Dec. 1969, pp. 513-516.

NASA-Langley, 1971 —— 33 E-6391

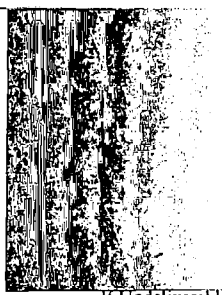

"The aeronautical and space activities of the United States shall be conducted so as to contribute . . . to the expansion of human knowledge of phenomena in the atmosphere and space. The Administration shall provide for the widest practicable and appropriate dissemination of information concerning its activities and the results thereof."

—NATIONAL AERONAUTICS AND SPACE ACT OF 1958

NASA SCIENTIFIC AND TECHNICAL PUBLICATIONS

TECHNICAL REPORTS: Scientific and technical information considered important, complete, and a lasting contribution to existing knowledge.

TECHNICAL NOTES: Information less broad in scope but nevertheless of importance as a contribution to existing knowledge.

TECHNICAL MEMORANDUMS: Information receiving limited distribution because of preliminary data, security classification, or other reasons.

CONTRACTOR REPORTS: Scientific and technical information generated under a NASA contract or grant and considered an important contribution to existing knowledge.

TECHNICAL TRANSLATIONS: Information published in a foreign language considered to merit NASA distribution in English.

SPECIAL PUBLICATIONS: Information derived from or of value to NASA activities. Publications include conference proceedings, monographs, data compilations, handbooks, sourcebooks, and special bibliographies.

TECHNOLOGY UTILIZATION PUBLICATIONS: Information on technology used by NASA that may be of particular interest in commercial and other non-aerospace applications. Publications include Tech Briefs, Technology Utilization Reports and Technology Surveys.

Details on the availability of these publications may be obtained from:

SCIENTIFIC AND TECHNICAL INFORMATION OFFICE

NATIONAL AERONAUTICS AND SPACE ADMINISTRATION

Washington, D.C. 20546